



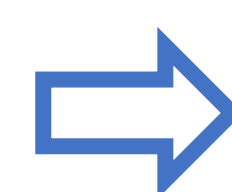
## Introduction

Airborne radionuclide measurements are being made routinely by the International Monitoring System, which is being setup to detect signatures of possible violations of the Comprehensive Nuclear-Test-Ban Treaty. To obtain information on the source of any detected radionuclides, inverse atmospheric transport modelling can be used. Different inverse modelling approaches have been proposed, but studies are often limited to specific

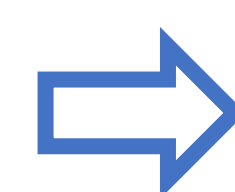
case studies, making it hard to get insight in its performance when applied to future cases of interest. In this study, we apply inverse modelling to 36 time-consecutive case studies, using Xe-133 detections originating from a major medical isotope production facility. The objective is to get more insight in the inverse modelling method used in [1,2].

## Inverse modelling:

Detections and non-detections ( $y$ ) taken at RN16, RN17, RN74 and RN75  
Month1: 1-15<sup>th</sup>  
Month2: 16<sup>th</sup>-end of month



Source-receptor-sensitivities ( $M$ ) made available by the PTS (Flexpart-ECMWF)



A source term  $x_j$  is found by minimizing a cost function (with  $\alpha$  the MDC):

$$\exp\left(\frac{1}{n} \sum_i (\log(y_i + \alpha) - \log(M_{ij}x_j + \alpha))^2\right)$$

The optimisation is solved using a quasi-Newton technique and does not require to rerun Flexpart

## Results

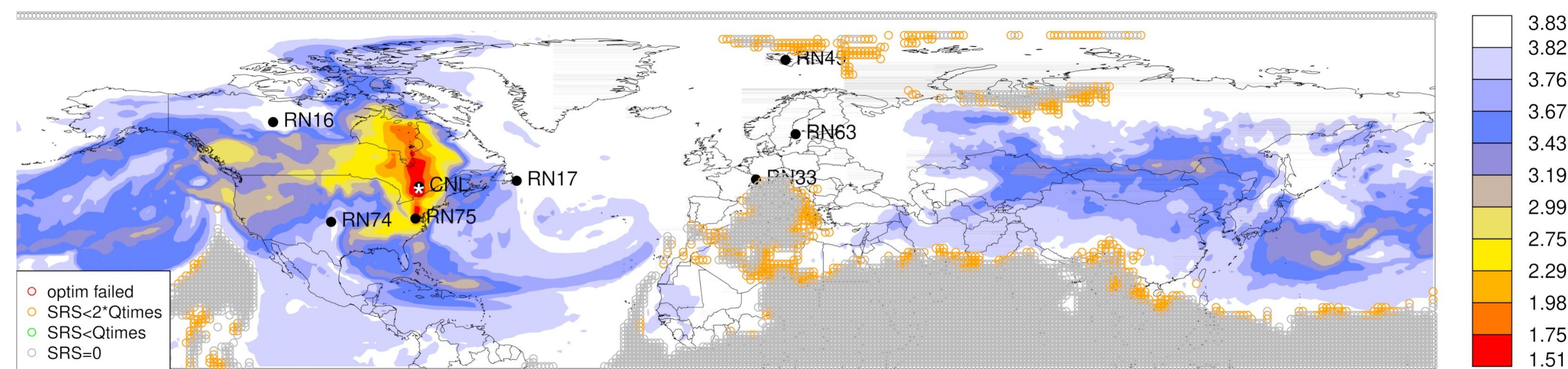


Fig. 1: Map with the cost function values for each grid box in the lowest model level. Grid boxes with low cost function values can well explain the observations and can be considered as possible source regions (case Jun1 2014 as an example)

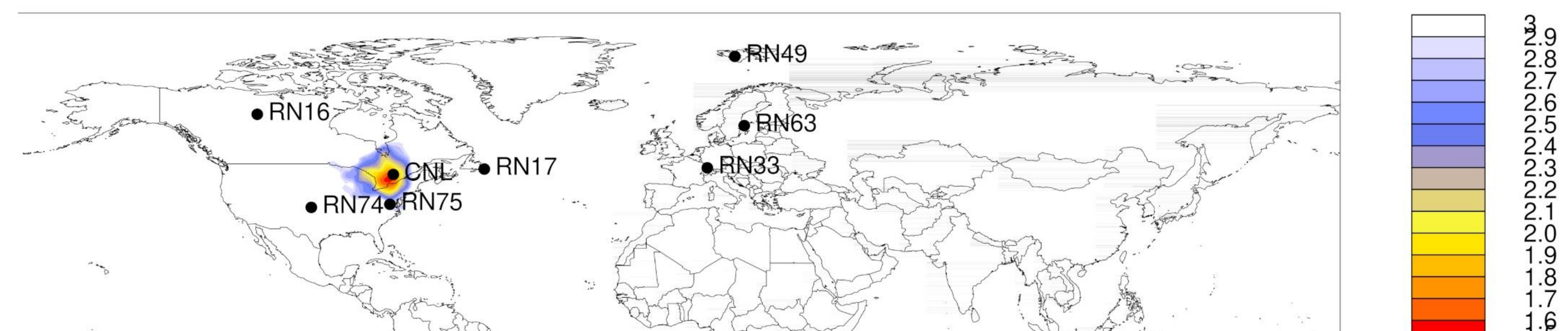


Fig. 2: Mean grid box cost function for all 36 cases. The region with the lowest cost function is centered around CNL (Canadian Nuclear Laboratories)

Fig. 3: The relatively large number of cases allows to test different inverse modelling settings and quantify its performance. Mean and median distance for all cases between CNL and the grid box with the minimum cost value, using two cost functions: mean square error (mse) and geometric variance (VG) for 1, 2, 4 or 8 release intervals.

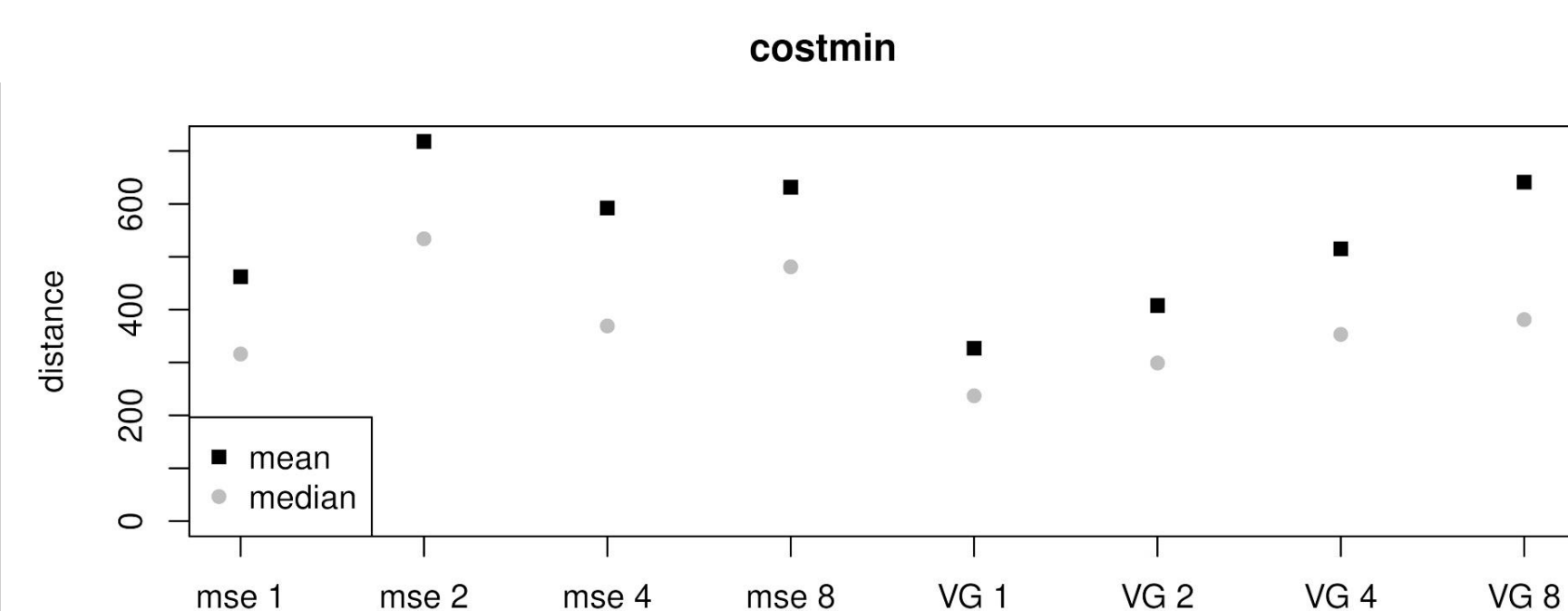
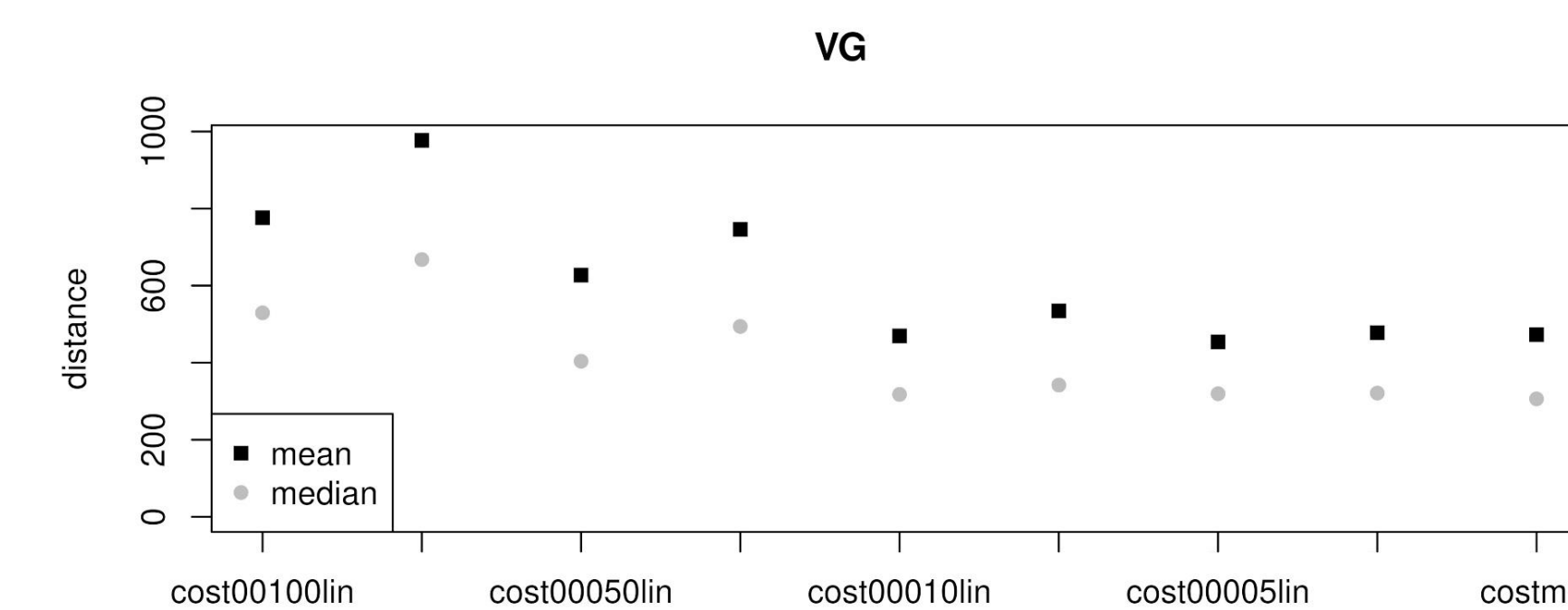


Fig. 4: Results using the geometric variance (VG) and 1 release interval (that is, a continuous release). Mean and median distance between CNL and different source location estimators; *cost00100lin*: based on 1% lowest cost value grid boxes and using linear weights based on the cost function.



## Conclusions

- The high quality radioxenon measurements made routinely by the IMS, combined with knowledge of major radioxenon emitters has the potential (1) to help validate inverse atmospheric modelling techniques and (2) to assess its performance under various conditions.
- The performance of different techniques can be quantified, in order to improve existing inverse modelling techniques.
- Unknown radioxenon sources of which its signature is detected regularly by the IMS can be located more accurately by aggregating the analysis of many detections taken at different periods.

## References

- [1] De Meutter, P., Camps, J., Delcloo, A., & Termonia, P. (2017). Assessment of the announced North Korean nuclear test using long-range atmospheric transport and dispersion modelling. Scientific reports, 7(1), 8762.
- [2] De Meutter, P., Camps, J., Delcloo, A., & Termonia, P. (2018). Source localisation and its uncertainty quantification after the third DPRK nuclear test. Scientific reports, 8(1), 10155.

Period	Distance	Quantile
Jun1 2014	39	0.999
Jun2 2014	580	0.998
Jul1 2014	128	0.999
Jul2 2014	546	0.999
Aug1 2014	556	0.992
Aug2 2014	194	0.999
Sep1 2014	39	0.999
Sep2 2014	231	0.999
Oct1 2014	298	0.999
Oct2 2014	306	0.999
Nov1 2014	117	0.999
Nov2 2014	562	0.999
Jan1 2015	359	0.999
Jan2 2015	1395	0.996
Feb1 2015	901	0.996
Feb2 2015	431	0.999
Mar1 2015	170	0.999
Mar2 2015	1252	0.999
Apr1 2015	262	0.999
Apr2 2015	41	0.999
May1 2015	1037	0.999
May2 2015	240	0.999
Jun1 2015	305	0.999
Jun2 2015	2422	0.999
Jul1 2015	41	0.995
Jul2 2015	237	0.999
Aug1 2015	128	0.999
Aug2 2015	41	0.999
Sep1 2015	129	0.999
Sep2 2015	129	0.999
Oct1 2015	237	0.999
Oct2 2015	129	0.999
Nov1 2015	471	0.999
Nov2 2015	348	0.999
Dec1 2015	107	0.998
Dec2 2015	169	0.998